Nanoliter-Droplet Acoustic Streaming via Ultra High Frequency Surface Acoustic Waves

Richie J. Shilton, Marco Travagliati, Fabio Beltram, and Marco Cecchini**

A fundamental limitation within the field of digital microfluidics is the minimum droplet volume that can be internally-controlled and exploited. Surface acoustic waves (SAWs) have been shown to be a fast and efficient method for generating internal flows and patterning in microfluidic droplets, but no improvements in droplet miniaturization have been reported since its introduction. Here we demonstrate the relevant length scales in sub-nanometer amplitude SAW-driven acoustic streaming. We illustrate the absence of any physical limitations beyond fabrication capabilities preventing the downscaling of SAW-driven internal streaming to nanoliter microreactors and beyond, and we experimentally demonstrate this by extending SAW microfluidics up to operating frequencies in the GHz range. The scaling is applied to demonstrate ultrafast fluid mixing in nanoliter order droplets by exploiting 1.1 GHz SAW.

Development of micro-total-analysis systems offers new possibilities in portable healthcare and environmental sensor systems. SAW driven microfluidics has become a very powerful fluid actuation method owing to the ability of SAWs to transfer a large amount of momentum into fluids, using integrated transducers in truly portable battery-operated systems.[1] The typical amplitudes of SAWs used in these devices are on the order of nanometers or less, however owing to the high frequencies used (O(10 – 100 MHz)) the accelerations induced by these waves are enormous—over 10^7 ms^{-2}—which can be exploited to drive ultra-fast flows in microfluids.[2] Depending on geometry and power input, SAWs can actuate a range of fluid processes such as mixing,[3,4] particle manipulation,[5–7] droplet actuation,[8–10] atomization,[11] water-in-oil emulsions,[12] and pumping in closed microchannels via acoustic counterflow.[13,14] Digital SAW microfluidics applications have typically been demonstrated using microliter droplets or larger, as in the case of other digital microfluidics technologies.[15] Further miniaturization beyond these limits, including fine control of internal flows in nanoliter order microreactors, is imperative to address as we look to the future of digital microfluidics.

The outstanding performance of SAW-driven micro-mixers, micro-centrifuges and micro-sorters[5] arises from SAW-driven acoustic streaming. SAWs radiate acoustic energy into fluids owing to the sound velocity mismatch between the fluid and the substrate. The induced pressure wave in turn drives a steady state flow, namely acoustic streaming. Up to now SAW microfluidic devices have typically been operated with frequencies between 20 MHz to 200 MHz, with acoustic wavelengths above ~20 μm (although they have been exploited very recently up to ~300 MHz[16,17]). No scaling laws of the resulting flow patterns as a function of the acoustic length scales has been explicitly investigated. In order to downscale SAW microfluidics, we have studied for the first time here acoustic streaming and particle patterning as a function of the operating SAW frequency from 47.8 – 1107 MHz while varying the droplet volumes from microliters down to ≲ 1 nanoliter. We demonstrate how acoustic streaming and particle patterning scales with the ratio of droplet sizes to viscous fluid acoustic damping and SAW damping lengths. For the first time acoustic streaming and ultrafast mixing in nanoliter order droplets is investigated by exploiting SAWs in the ultra high frequency range (UHF; defined as 300 MHz – 3 GHz).

SAW microfluidic devices, as shown in **Figure 1**, were fabricated at nominal frequencies of 50, 100, 200, 400, 833, and 1250 MHz, and the reflection coefficients were measured to find the resonant frequency at which to operate (**Table 1**; details of similar fabrication techniques can be found in Travagliati et al.[18]). Each SAW device consisted of straight-fingered titanium:gold (10 nm:100 nm) interdigital transducers (IDT) patterned on 128° Y-cut, X-propagating lithium niobate (LN) substrates. For the purpose of microfluidic actuation, the amplitude of the SAWs generated by each device was set to A = 100 pm by direct measurement with a laser Doppler vibrometer (LDV; UHF-120 Ultra High Frequency Vibrometer, Polytec, Germany). The SAW amplitude was measured in the region where the fluid was placed, and was found to be consistent across the wave path. To visualize internal streaming flows, droplets were pinned in hydrophilic well regions formed by patterned surface silanes. The contact angle for each droplet on the surface was 93° ± 3°. For the case of the large droplets in **Figure 2** only, a coverslip was placed over the droplets with 385 μm spacers to aid in flow visualization. Similar setups were used to demonstrate microfluidic mixing, with initially segregated fluid

Dr. R. J. Shilton
Center for Nanotechnology Innovation@NEST
Istituto Italiano di Tecnologia
Piazza San Silvestro 12, 56127, Pisa, Italy
E-mail: richard.shilton@iit.it
M. Travagliati, Prof. F. Beltram
Center for Nanotechnology Innovation@NEST
Istituto Italiano di Tecnologia
Piazza San Silvestro 12
56127, Pisa, Italy
M. Travagliati, Prof. F. Beltram
NEST, Scuola Normale Superiore and Istituto Nanoscienze-CNR
Piazza San Silvestro 12, 56127, Pisa, Italy
Dr. M. Cecchini
NEST, Scuola Normale Superiore and Istituto Nanoscienze-CNR
Piazza San Silvestro 12, 56127, Pisa, Italy
E-mail: marco.cecchini@nano.cnr.it

DOI: 10.1002/adma.201400091

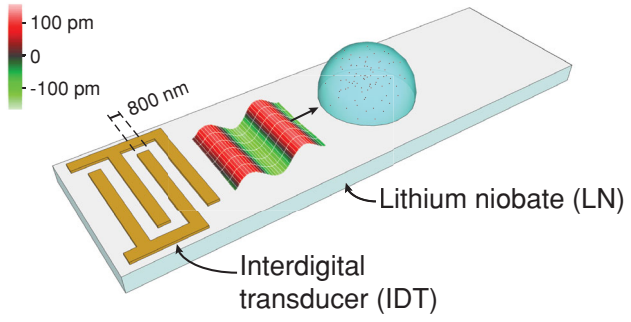

Figure 1. Schematic of the 1.1 GHz surface-acoustic-wave microfluidic device (not to scale). An overlaid section of a representative LDV (laser Doppler vibrometer) measurement shows a 100 pm amplitude SAW travelling from the IDT to the fluid droplet.

sections. For 1 μL droplets 10% dye was initially compartmentalized in water, and for the nanoliter scale droplets latex beads (500 nm) were used. Mixing efficiency was determined by a normalized mixing index over time, with an associated mixing half-life (details in Ref. [4]).

Figure 2 shows the flow streamlines (from overlaid images of particle tracers) of representative measurements for the different operating frequencies used to actuate internal streaming in 1 μL particle seeded water droplets of diameter d = 1.5 mm. A frequency dependent transition between two distinct flow patterns was seen as the frequency was increased. Streamlines with standard double vortical structures[19] were observed for the droplets actuated by resonant frequencies up to 374 MHz. While this flow structure was apparent at frequencies that are typically associated with SAW microfluidics, at frequencies above 374 MHz a different flow structure appeared. This new flow pattern was characterized by two regions; one at the leading edge and one at the rear of the droplet. In the front region, again, there was a symmetrical vortical pattern with a strong three dimensional (3D) structure in which particles move upwards away from the SAW scattering region. The back region instead was characterized by a single rolling motion. As the frequency was increased from 752 MHz to 1.107 GHz the front vortices were compressed further and the back-rolling motion had the appearance of becoming increasingly chaotic.

The flow pattern transition can be described in terms of the decreased damping length of the acoustic wave in a viscous fluid, x_f, as the frequency was increased. The damping length of an acoustic wave in water is given by $x_f = 1/(\gamma k_f)$, where $k_f = \omega/c_f$ and γ is $(1+\beta)\eta\omega/(2\rho_f c_f^2)$, where γ is the non-dimensional acoustic damping factor, c_f is the speed of sound in fluid, β is the non-dimensional viscosity ratio (5/3 for simple fluids such as water), and η is the kinematic viscosity[20]—given for each frequency in Table 1. The standard vortex pairs were generated by the 47.9 – 374 MHz devices, where x_f was greater (or on the order of) the droplet height h. For the devices with frequencies above 374 MHz, where there was the new strongly 3D fluid flow, the acoustic wave in the fluid died out at a decreasing fraction of the droplet size. The standard dual vortex flows can be expected for cases where $h/x_f < 1$ and the new compartmentalized 3D pattern will occur in cases of $h/x_f > 1$. Where $h < x_f$, a significant part of the acoustic energy was reflected at the surface of the droplet, generating a pressure field over the droplet length which induced a jet extension (central high velocity fluid path) over the entire droplet as in the standard pattern. Conversely, where $h > x_f$ the acoustic wave energy was dissipated before reflection at droplet surface and a strong gradient was defined only in the front region of the droplet. We in turn saw the jet and vortex pairs (the region of most intense fluid velocities) withdrawing closer to the fluid front—a change from the two-dimensional flows of lower frequency devices previously studied. Here, the pressure wave was compressed in the front region and its gradient was stronger in the out-of-plane direction. In the rear of the droplets where there was the single-rolling motion, instead, the pressure field had almost vanished. As the frequency was increased from 752 MHz to 1.107 GHz the back-rolling motion had the appearance of becoming increasingly chaotic. This may be expected as the acoustic intensity radiated into the droplet scales as $I \sim f^2A^2$ and it has been shown that at a fixed low frequency an increase of acoustic power leads to an increase of chaos in the flow structure.[4,5]

Figure 3 demonstrates downscaling of the SAW microfluidic technology (Video S1). Flow patterns inside three significantly smaller nanoliter order droplets actuated by four frequencies are shown; (a) 47.8 MHz, (b) 94.9 MHz, (c) 191 MHz and (d) 1107 MHz (water seeded with 500 nm particles; 374 MHz and 752 MHz are not shown as they were qualitatively similar to 1107 MHz). For each droplet in the 47.8 MHz case (Figure 3(a)), there was a departure from the vortical structure seen in Figure 2 and particles accumulated in rings as standing waves were formed in the droplet, reminiscent of Li

Table 1. Properties of the SAW devices used.

Frequency, nominal f_0 [MHz]	Frequency, actual f [MHz]	Wavelength, λ_s [μm]	Damping length, water x_f [mm]	Damping length, SAW x_s [μm]
50	47.8	80	27.1	463
100	94.9	40	6.89	233
200	191	20	1.7	106
400	374	10	0.44	59
833	752	4.8	0.11	29
1250	1107	3.2	0.05	20

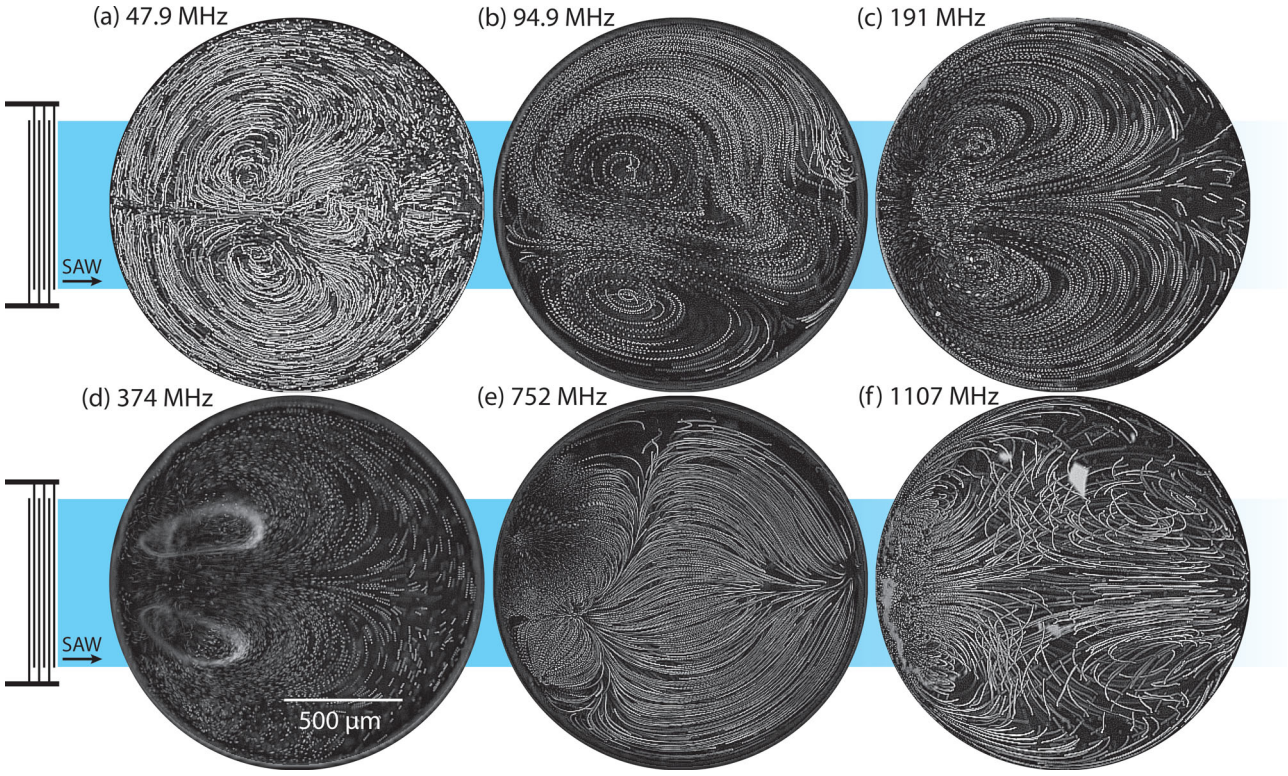

Figure 2. Streamlines of internal acoustic streaming shown for each SAW frequency (1 µL water droplets seeded with 5 µm particles). For each case, 25–200 frames were overlaid, depending on the speed of the particles for best visualization. The SAW direction is to the right, as indicated, and the aperture and vertical position of the IDTs is shown to scale with respect to the droplet size.

et al.'s pattern generation in larger droplets by low (20 MHz) frequency SAW.[21] For the 94.9 MHz and 191 MHz induced flows there was a transition from the vortical structure seen in the larger droplet (and in Figure 2) to ring-patterns of the particles in the smaller droplets. The 94.9 MHz driven flows in the 26 nL droplet (Figure 3(b) left) and the 191 MHz driven flows in the 6.6 nL droplet (Figure 3(c) center) both exhibited transitional behaviors, displaying a combination of dual vortices and standing waves. For the 1107 MHz case (Figure 3(d)), the standard pair of vortices formed again in each case, demonstrating acoustic streaming flow in the 1.2 nL droplet. The smallest droplets in Figure 3(a–c) also showed that the distance between the standing wave driven accumulation lines decreased with the decrease in acoustic wavelength (increase in operating frequency). By adjusting the frequency of operation within this range, particle positioning and patterning could be controlled.

This streaming-to-particle accumulation transition above can be described in terms of the droplet size d compared to the SAW damping length, $x_s = 0.45\ \lambda_s\ (\rho_s c_s)/(\rho_f\ c_f)$ where λ_s, ρ_s and c_s are the wavelength, density and speed of the SAW in the substrate respectively.[22] Acoustic streaming is generated when $d/x_s > 1$, while particle accumulation lines occur when $d/x_s \ll 1$. At the transition $d/x_s \sim 1$, particle dynamics resulting in a combination of the two cases occurs. When $x_s \ll d$ the acoustic source at the substrate-fluid interface has a substantial gradient, typical of previous SAW digital microfluidics investigations. If, however, $x_s > d$, the acoustic field in the substrate at the solid-liquid interface has minimal decay over the droplet length resulting in an acoustofluidics behavior similar to bulk acoustic wave (BAW) actuated devices where standing waves appear in the fluid. In this situation particle accumulation along anti-nodal lines dominates over the acoustic streaming as has been theoretically shown for fluid reactor geometries with aspect ratios of less than two.[23,24]

We now exploit the UHF-SAW driven streaming results from the previous sections to demonstrate one of the most important, difficult and limiting aspects of microfluidics—efficient and fast fluid mixing in microdroplets. **Figure 4**(a) shows the mixing half-lives for 1 µL droplets over the investigated range of frequencies (as in Figure 2). We find that fast mixing is obtained for all the tested frequencies. Mixing times (M_τ) are reduced by increasing the SAW frequency while keeping the SAW amplitude (A = 100 pm) constant, and scales as $M_\tau \sim f^{-2}$. This is a convenient scaling law and shows that M_τ scales with the inverse of the acoustic intensity, I, with a slight deviation at the highest frequency, possibly owing to some of the energy being used to generate droplet atomization.[11] The truly impacting application, however, is shown in Figure 4(b)–(d), where we apply the 1.1 GHz generated streaming to drive mixing in nanoliter order droplets. As shown in Figure 3, standing wave patterns and particle accumulations are generated in nanoliter scale droplets at typical SAW frequencies, which are not beneficial for mixing. Here, we instead exploit the UHF regime of acoustic streaming to generate mixing flows in these very small droplets. Figure 4(b) and (c) shows typical comparison images over time between mixing in a ~6 nL droplet via (b) diffusion

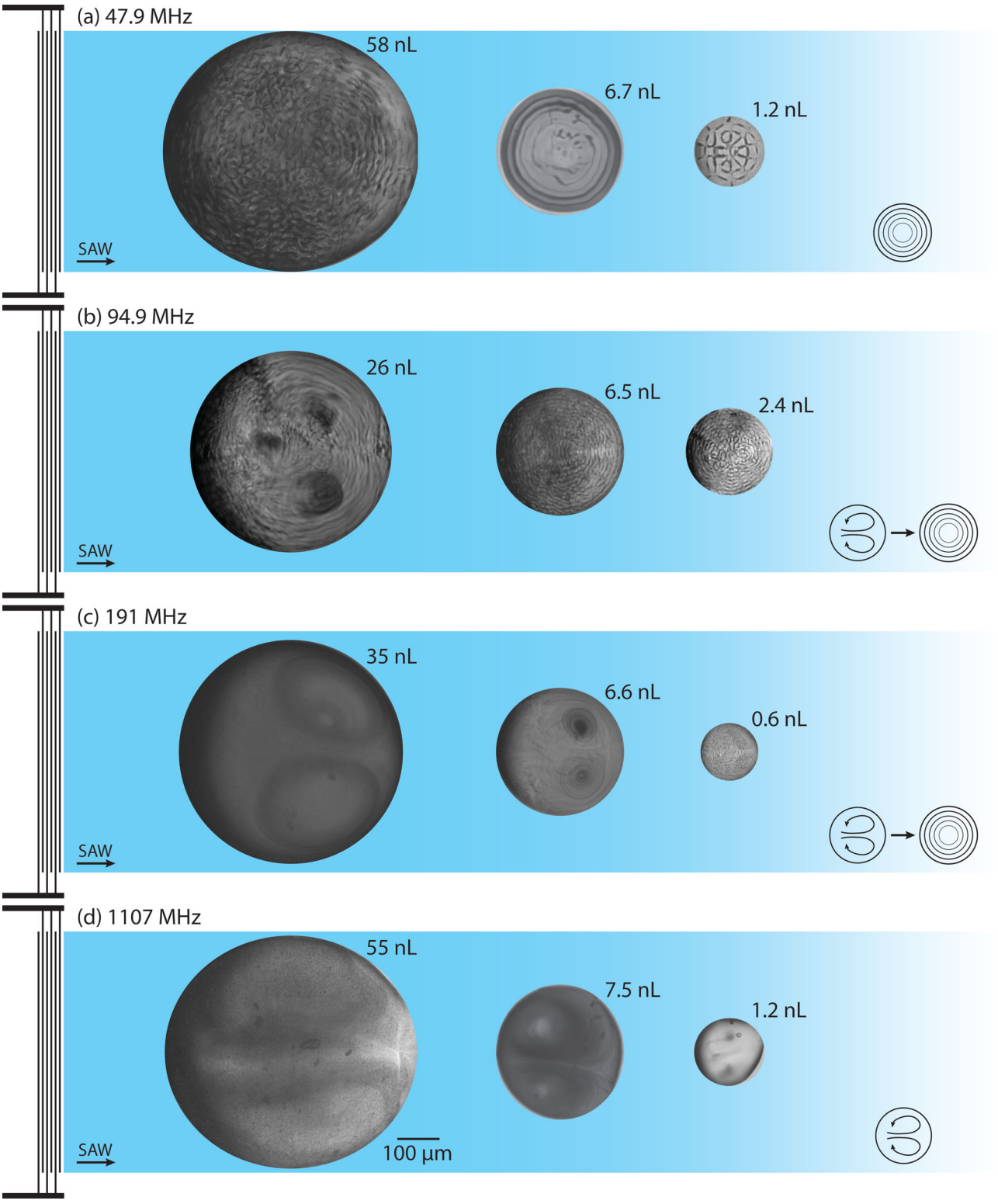

Figure 3. Acoustic streaming within nanoliter order free droplets actuated by (a) 47.8 MHz, (b) 94.9 MHz, (c) 191 MHz, and (d) 1107 MHz SAW. In the (a) 47.8 MHz case we see particles accumulating in patterns and rings as standing waves are formed in the droplets. The (b) 94.9 MHz, and (c) 191 MHz cases show transitional regions where the larger droplet exhibits streaming, with particle aggregations beginning to dominate as the drop volume decreases. For the (d) 1107 MHz case, however, we see the standard vortical streaming pairs forming in each droplet size.

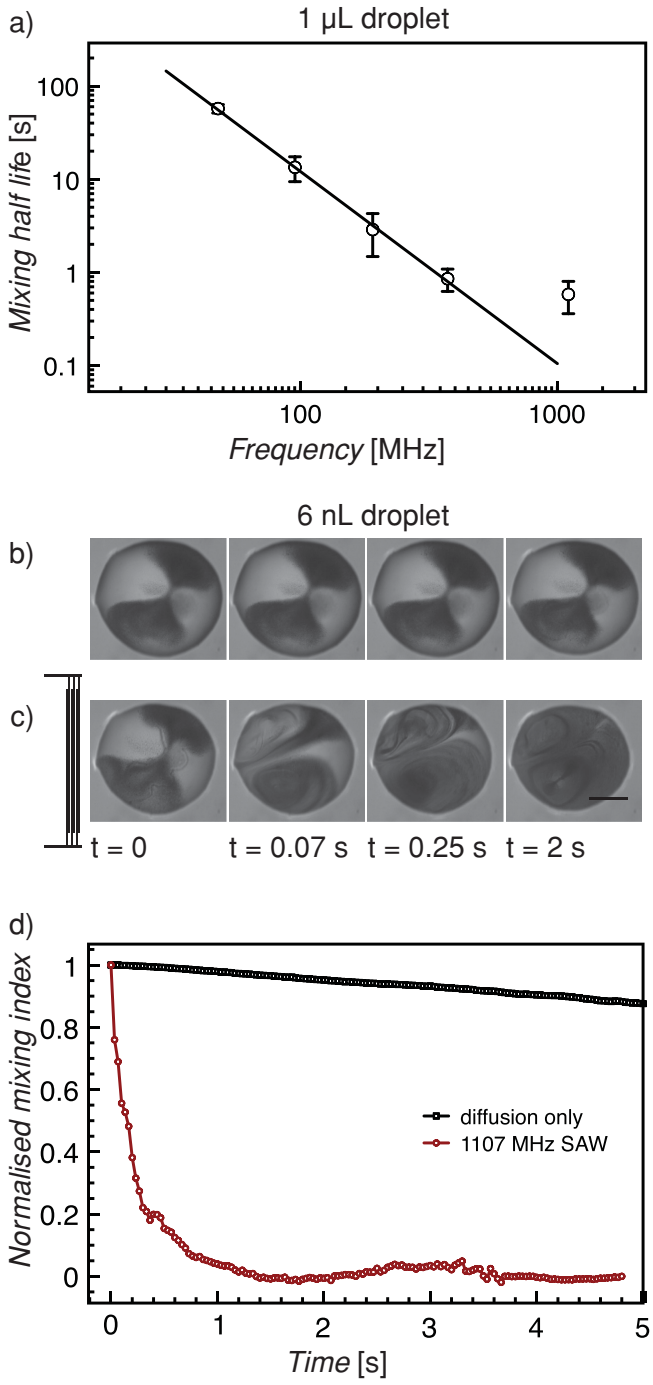

Figure 4. Active digital microfluidic mixing driven by ultra high frequency acoustic streaming. For typical 1 µL droplets (a) mixing half-lives are shown over the range of frequencies, and scale as $M_\tau \sim f^{-2}$ (black line). Mixing is shown for a ~6 nL droplet via (b) diffusion only, and actuated via a (c) 1107 MHz SAW. For nanoliter order droplets a shift to the UHF region is necessary to induce streaming. The normalized mixing of (b) and (c) are shown over time in (d), and shows a dramatic decrease in mixing time of over 100 times when the SAW is applied. Scale bar is 100 µm.

alone, and (c) 1.1 GHz SAW driven acoustic streaming. We see a dramatic decrease in mixing time of over two orders of magnitude.

In conclusion, we demonstrated that the necessary condition for vortical streaming in nanoliter volume droplets is $x_s \ll d$, where there is a sufficient pressure gradient to initiate acoustic streaming rather than standing wave patterns. Additionally, as x_f becomes significantly small with respect to the droplet diameter the vortical patterns compress to the leading edge and the bulk flow becomes increasingly chaotic and three dimensional. By increasing the frequency of operation we can restore the standard SAW patterns that we see at lower, common operating frequencies, but now in significantly smaller droplets—microliters can in this way be reduced to nanoliters. By accessing frequencies up to the GHz range as shown here, tailored internal flow patterns can be induced in much smaller fluid droplets than were previously available by other microfluidic methods. This was applied to demonstrate a reduction of over two orders of magnitude in mixing time in nanoliter order droplets as compared to diffusion alone. Acoustic streaming patterns and mixing in nanoliter free-droplets are shown, which can be exploited for nano-fluidic mixers and particle manipulations, and extended to new types of flows and pattern generations in micro-channels for lab-on-a-chip devices.

Supporting Information

Video: *Nanoliter droplet acoustic streaming and particle accumulation is available* from the Wiley Online Library or from the author.

Acknowledgements

This work has been supported in part by the CNR project: NANOMAX "Nanotechnology-based therapy and diagnostics of brain diseases – NANOBRAIN".

Received: January 7, 2014
Revised: February 24, 2014
Published online: March 27, 2014

[1] J. Friend, L. Y. Yeo, *Rev. Mod. Phys.* **2011**, *83*, 647.
[2] L. Y. Yeo, J. R. Friend, *Annu. Rev. Fluid Mech.* **2014**, *46*, 379.
[3] A. Wixforth, C. Strobl, C. Gauer, A. Toegl, J. Scriba, Z. v. Guttenberg, *Anal. Bioanal. Chem.* **2004**, *379*, 982.
[4] R. J. Shilton, L. Y. Yeo, J. R. Friend, *Sens. Actuators, B* **2011**, *160*, 1565.
[5] R. Shilton, M. K. Tan, L. Y. Yeo, J. R. Friend, *J. Appl. Phys.* **2008**, *104*, 014910.
[6] N. D. Orloff, J. R. Dennis, M. Cecchini, E. Schonbrun, E. Rocas, Y. Wang, D. Novotny, R. W Simmonds, J. Moreland, I. Takeuchi, *Biomicrofluidics* **2011**, *5*, 044107.
[7] J. Neumann, M. Hennig, A. Wixforth, S. Manus, J. Radler, M. Schneider, *Nano Lett.* **2010**, *10*, 2903.
[8] S. Shiokawa, Y. Matsui, T. Ueda, *Liquid streaming and droplet formation caused by leaky Rayleigh waves. Ultrasonics Symposium*, Proceedings., IEEE **1989**, pp 643–646.
[9] M. Travagliati, G. De Simoni, C. M. Lazzarini, V. Piazza, F. Beltram, M. Cecchini, *Lab Chip* **2012**, *12*, 2621.
[10] M. Alghane, Y. Fu, B. Chen, Y. Li, M. Desmulliez, A. Walton, *Microfluid. Nanofluid.* **2012**, *13*, 919.
[11] M. Kurosawa, A. Futami, T. Higuchi, *Characteristics of liquids atomization using surface acoustic wave. Solid State Sensors and Actuators,*

TRANSDUCERS'97 Chicago., International Conference on. **1997**, pp 801–804.
[12] D. J. Collins, T. Allen, K. Helmerson, A. Neild, *Lab Chip.* **2013**, *13*, 3225.
[13] M. Cecchini, S. Girardo, D. Pisignano, R. Cingolani, F. Beltram, *Appl. Phys. Lett.* **2008**, *92*, 104103.
[14] L. Masini, M. Cecchini, S. Girardo, R. Cingolani, D. Pisignano, F. Beltram, *Lab Chip* **2010**, *10*, 1997.
[15] K. Choi, A. H. Ng, R. Fobel, A. R. Wheeler, *Annu. Rev. Anal. Chem.* **2012**, *5*, 413.
[16] V. Skowronek, R. Rambach, L. Schmid, K. Haase, T. Franke, *Anal. Chem.* **2013**, *85,* 9955.
[17] M. Dentry, J. Friend, L. Yeo, *Lab Chip* **2014**, *4*, 750.
[18] M. Travagliati, R. Shilton, F. Beltram, M. Cecchini, *JoVE* **2013**, *78*, e50524.
[19] Z. Guttenberg, A. Rathgeber, S. Keller, J. Rädler, A. Wixforth, M. Kostur, M. Schindler, P. Talkner, *Phys. Rev. E* **2004**, *70*, 056311.
[20] H. Bruus, *Theoretical microfluidics*, Oxford University Press, New York **2007**, Vol. *18*.
[21] H. Li, J. R. Friend, L. Y. Yeo, *Phys. rev. lett.* **2008**, *101*, 084502.
[22] T. Frommelt, D. Gogel, M. Kostur, P. Talkner, P. Hanggi, A. Wixforth, *Ultrasonics, Ferroelectrics and Frequency Control, IEEE Transactions on* **2008**, *55*, 2298.
[23] P. B. Muller, R. Barnkob, M. J. H. Jensen, H. Bruus, *Lab Chip* **2012**, *12*, 4617.
[24] R. Barnkob, P. Augustsson, T. Laurell, H. Bruus, *Phys. Rev. E* **2012**, *86*, 056307.